

Revisited vibrational assignments of imidazolium-based ionic liquids

Joseph Grondin,^{a*} Jean-Claude Lassègues,^a Dominique Cavagnat,^a Thierry Buffeteau,^a Patrik Johansson^b and Roman Holomb^c



Imidazolium-based ionic liquids (ILs) involving anions of variable coordinating strength have been investigated using infrared (IR) and Raman spectroscopies, density functional theory (DFT) calculations and selective deuteration of the imidazolium CH groups. Particular emphasis has been placed on the vibrational assignments of the anion and cation internal vibrations, a prerequisite before any interpretation of spectral changes due to ion–ion interactions in these unconventional liquids. The vibrations of highly symmetric and weakly coordinating anions, such as PF_6^- , have unperturbed wavenumbers, but unexpected IR or Raman activity for some modes, showing that the anion is subjected to an anisotropic electric field. The stretching as well as the in-plane and out-of-plane bending modes of the imidazolium CH groups are anharmonic. They give broad bands that reflect a large distribution of interactions with the surrounding anions. All the bending modes are mixed with ring vibrations and the stretching modes are complicated by Fermi resonance interactions with overtones and combination of in-plane ring modes. However, the stretching vibration of the quasi-diatomic $\text{C}_{(2)}-\text{D}$ bond appears to be a good spectroscopic probe of the increasing cation–anion interactions when the coordinating strength of the anion increases. The broad absorption observed in the far IR with weakly coordinating anions remains practically unchanged when the acidic $\text{C}_{(2)}-\text{H}$ imidazolium bond is methylated and even when the imidazolium cation is substituted by tetra-alkyl ammonium or pyrrolidinium cations. It is concluded that this absorption is a general feature of any IL, coming from the relative translational and librational motions of the ions without needing to invoke $\text{C}_{(2)}-\text{H}$ anion hydrogen bonds. Copyright © 2010 John Wiley & Sons, Ltd.

Supporting information may be found in the online version of this article.

Keywords: ionic liquid; imidazolium; infrared; Raman; DFT

Introduction

Ionic liquids (ILs) are materials of increasing importance in many application fields.^[1,2] In addition to their intrinsic properties of solvation and of ionic conduction, they offer unexpected possibilities in domains such as bioscience or biomechanics. However, the understanding of the nature of the ion–ion interactions, which is a prerequisite for future rational developments of more complex IL-based systems, has not progressed at the same speed and is still largely elusive. Among the huge number of experimental and theoretical methods applied to unravel the fundamental aspects, infrared (IR) and Raman spectroscopies, generally together with density functional theory (DFT) calculations, bring their own specific contribution by trying to interpret spectral features in terms of the internal and external structure and dynamics of the IL anions and cations.^[3–25] External motions, i.e. relative translational and librational motions of the cations and anions, are revealed in the spectral region below about 150 cm^{-1} in the form of a broad absorption band.^[26–33] It is particularly important to measure quantitatively the far-IR response to connect it to terahertz dielectric and conductivity results.^[34–38] Indeed, the ILs' dielectric properties have to be unravelled over a wide frequency, and hence time, domain for a better understanding of the local structure and dynamics. However, most spectroscopic studies have been devoted to the intramolecular vibrations of the cations and anions. Important progress was made in the determination of the conformational states of 1,3 disubstituted imidazolium cations such as 1-ethyl-3-methyl imidazolium (EMI^+) or 1-butyl-3-methyl imidazolium (BMI^+),^[8,16,17] and similarly for

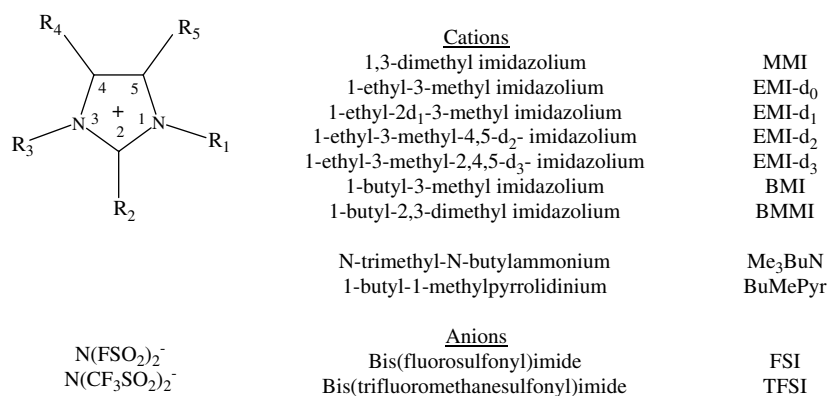
anions such as bis(trifluoromethylsulfonyl)imide (TFSI^-), all defined in Scheme 1.^[9–11,16] Then, the spectral perturbations of some oscillators were investigated as a function of various parameters (temperature, pressure, dissolution in different solvents) and tentatively associated to specific cation–anion interactions.^[12,15,38–41] A classical example is the $\text{C}_{(2)}\text{H}$ group of 1,3 alkyl-disubstituted imidazolium cations (Scheme 1), likely to establish $\text{CH}\cdots$ anion hydrogen bonds.^[12,15] However, the IR and Raman spectra of the imidazolium CH stretching vibrations (νCH) has proved difficult to interpret and led to several contradictory assignments in the literature.^[25,42–44] It is now obvious that the νCH region cannot be analysed alone without considering all the other internal vibrations of the cation. Therefore, we have decided to use the classic method of H/D isotopic substitution, along with DFT calculations, to achieve a better assignment of the cation vibrations. Furthermore, to evaluate the role of the $\text{C}-\text{H}\cdots$ anion interactions in imidazolium-based ILs, a series of anions have been considered,

* Correspondence to: Joseph Grondin, ISM, UMR 5255, CNRS, Université Bordeaux I, 351 Cours de la Libération, 33405 Talence Cedex, France.
E-mail: j.grondin@ism.u-bordeaux1.fr

a ISM, UMR 5255, CNRS, Université Bordeaux I, 33405 Talence Cedex, France

b Department of Applied Physics, Chalmers University of Technology, SE-41296 Göteborg, Sweden

c Institute of Solid State Physics and Chemistry, Uzhhorod National University, Uzhhorod, Ukraine



Scheme 1. Nomenclature used for the investigated cations and for some associated anions.

from the weakly coordinating TFSI⁻, PF₆⁻ or BF₄⁻ to the more basic N(CN)₂⁻, SCN⁻, I⁻ and Br⁻.

In the following, the vibrations of these anions in various ILs are first briefly investigated. Then, the isotopic derivatives of 1-ethyl-3-methyl imidazolium (EMI) described in Scheme 1 are thoroughly compared with calculated spectra to establish a complete assignment of the vibrations occurring below 1600 cm⁻¹ and above 2800 cm⁻¹. Emphasis is placed on the cation vibrations that are likely to reveal differences between the 'free' state and situations where it is submitted to ionic interactions of variable strength. Finally, the intermolecular cation–anion vibrations observed in the far-IR are commented.

Materials and Methods

Materials

All the ILs used in this work and described in Scheme 1 were purchased from the Solvionic company at a purity of 99.9%. They were used as received, but always stored and handled in a dry box filled with argon. To help vibrational assignments, the three imidazolium CH bonds of the EMI⁺ cation were selectively deuterated in two typical ILs: the hydrophilic [EMI][Br] and the hydrophobic [EMI][TFSI]. Only the C₍₂₎–H bond was deuterated for other ILs.

Various methods of deuteration of the CH imidazolium groups have been proposed in the literature by adding bases,^[4,45–47] Lewis acids,^[48] metal clusters^[49] or even heterogeneous Pd catalysts.^[50] We have rather tried to perform selective H/D deuteration on the three imidazolium CH groups by introducing no other additive than the deuterated solvents D₂O or CD₃OD. Thereby, the deuteration process can be followed *in situ* by Raman spectroscopy while avoiding fluorescence effects and parasitic signals of added molecules or ions. Additionally, the liquid samples are contained in closed or sealed glass tubes and can therefore be examined at any time without having to extract and consume part of the solution and, in case of phase separation, also in the different phases directly.

[EMI][Br] was dissolved in D₂O according to the method described by Dieter *et al.*^[4] Molar ratios [EMI][Br]/D₂O varying from 1/5 to 1/100 were used. The C₍₂₎H groups are thus easily transformed into C₍₂₎D at room temperature to give the EMI-d₁ derivative. All the other CH bonds remain unchanged. Deuteration of the three CH groups to obtain the EMI-d₃ derivative is achieved by heating the [EMI][Br]/D₂O = 1/100 solution at 373 K during

several weeks. From EMI-d₃, it is then possible to obtain the EMI-d₂ derivative by exchanging D₂O by H₂O.

Deuteration of [EMI][TFSI] was also undertaken. As this compound is very sparingly soluble in water (1.8 wt.% at room temperature), it was first dissolved in CD₃OD. The EMI-d₁ derivative was obtained after a few hours at room temperature, but the C₍₄₎H and C₍₅₎H bonds could not be deuterated, even by heating the [EMI][TFSI]/CD₃OD solution at 393 K for a long time. [EMI][TFSI] was then sealed in a glass tube with D₂O and heated at 423 K during 2 weeks. The Raman spectrum of the lower non-aqueous phase indicated that the EMI-d₃ derivative was obtained, although again with ~90% yield. The EMI-d₂ derivative can then be obtained by exposing EMI-d₃ to CH₃OH.

The measurement of the deuteration rates by Raman spectroscopy is detailed below.

IR and Raman experiments

The Raman spectra were recorded with a Labram HR800 Jobin-Yvon spectrometer equipped with a krypton laser (752.45 nm), an air-cooled charge coupled device detector ANDOR and a 600 grooves mm⁻¹ grating giving a spectral resolution of 2 cm⁻¹. The ILs were contained in sealed or closed glass tubes for the Raman experiments. The IR spectra were recorded with a Thermo-Nicolet 6700 Nexus spectrometer at a resolution of 2 cm⁻¹ using an attenuated total reflection (ATR) accessory SPECAC equipped with a diamond or a germanium crystal. A very small quantity of liquid is needed to cover the ATR crystal (~10 μl), but this liquid must be protected from the ambient moisture. We have checked that the profiles of weak to medium intensity absorptions were not significantly perturbed by optical effects due to the low refractive index of the diamond crystal.^[24] However, ATR corrections are needed for strong absorptions, such as the antisymmetric vibrations of the BF₄⁻ or PF₆⁻ anions, which are highly distorted by the diamond device and to a lesser extent by the Ge device.^[24]

Computational methods

Harmonic *ab initio* vibrational calculations of the energy-minimised structures as well as the IR and Raman spectra, via second and third derivatives of the total energy, respectively, were carried out using the Gaussian03 software^[51] for various isotopic derivatives of the MMI⁺ and EMI⁺ cations and for the counter-anions separately. The DFT calculations were performed using the B3LYP functional^[52,53] with the 6-31G** basis set. In

addition to these standard type calculations, also anharmonic wavenumber calculations, using the vibrational self-consistent field (VSCF) strategy,^[54] were performed for the cations to provide the wavenumbers of the overtone and combination bands (Tables S1–6, Supporting Information). The coupling constants between two fundamentals or between fundamentals and overtones or combinations were previously calculated for the non-planar EMI⁺ cation.^[42] This was shown to be especially important to be able to address the complex ν CH region. For all calculated wavenumbers, scaling factors were applied locally to visualise the connection with the experimental data.

For MMI-*d*₀ and MMI-*d*₁, both of C_{2v} symmetry, the potential energy distribution (PED) for each mode in the harmonic approximation was determined according to the method developed by Allouche.^[55] The results are reported in Tables S1 and S2. Characteristic vibrations of the imidazolium ring can thus be evidenced and, in particular the three stretching vibrations ν CH (2A₁, B₂), the three in-plane bending modes δ CH (A₁, 2B₂), the three out-of-plane bending modes γ CH (A₂, 2B₁) and the nine ring vibrations (4A₁, 3B₂, 1A₂, 1B₁), in a very similar manner as previously done for the unsubstituted imidazolium cation.^[56] The ring vibrations, noted Rx (x = 1–9) for simplicity,^[56] involve complex motions. In the EMI⁺ derivatives, the imidazolium ring keeps a pseudo-C_{2v} symmetry and most of its characteristic vibrations are maintained. They can be followed from the PEDs calculated for the four EMI⁺ derivatives and reported in Tables S3–6.

Results and Discussion

The anion vibrations

Polyatomic anions such as SCN⁻, N(CN)₂⁻, B(CN)₄⁻, BF₄⁻, PF₆⁻ or N(CF₃SO₂)₂⁻ are frequently encountered in ILs. Their vibrational assignment is mostly documented in the literature.^[11,16,18,57–59] Here we would especially like to see whether some anion vibrational modes may be indicative of ion–ion interactions occurring in the ILs. As an example, the PF₆⁻ anion of octahedral symmetry has recently been shown to have its fully symmetric stretching, and thus IR inactive mode ν_1 , observed in the IR spectrum of liquid [EMI][PF₆].^[24] Similarly, the δ (BCN) bending mode of the tetrahedral B(CN)₄⁻ anion is observed in the Raman spectrum although it is Raman inactive for a strict T_d symmetry.^[18] Thus, these anions must be at least slightly perturbed. The wavenumbers of the observed anion vibrations in the IR and Raman spectra of [BMI][PF₆] (Table 1) indicate that there is no liftings of degeneracy or wavenumber shifts that could be interpreted by a lowering of the O_h symmetry to, e.g. a C_{4v} symmetry, as already reported for electrolytic solutions of alkali-metal cations when ion-pairing effects occur.^[58,59] The interactions of PF₆⁻ with the

surrounding imidazolium cations are weak enough to preserve a quasi-octahedral symmetry and the wavenumbers of a ‘free’ anion. It is clear, however, that the anion is subjected to long-range Coulombic interactions within the IL. In addition, these interactions have to be slightly anisotropic to explain the presence of the forbidden IR and Raman modes. For a better understanding of these activations, further results are reported in Fig. 1. In the IR spectra of [BMI][PF₆], the ν_1 mode of PF₆⁻ gives a weak absorption band at 740 cm⁻¹ on top of a broader absorption which will be identified later on as the out-of-plane vibration of the imidazolium C₍₄₎H and C₍₅₎H groups. By dilution in deuterated acetonitrile (CD₃CN), this ν_1 absorption vanishes (Fig. 1(a)), but in dimethylcarbonate (DMC) it persists and becomes even slightly more intense than in the pure IL (Fig. 1(b)). The intensity variation of the ν_1 band can be quantitatively evaluated using the 624 cm⁻¹ cation band as an internal reference (inserts of Fig. 1(a) and (b)). One can infer that solvents of low dielectric constant, such as DMC, solvate [BMI][PF₆] under the form of ion pairs (IPs), giving a maximum intensity to the ν_1 absorption, whereas more polar solvents (CD₃CN) solvate the ions separately to give solvent-separated ion pairs (SSIPs) in which the anion recovers the octahedral symmetry. At high dilution in CD₃CN, the ν_1 intensity goes to zero. However, a solvent such as propylene carbonate, of higher dielectric constant than CD₃CN, produces a decrease of the ν_1 intensity down to only ~0.07 at high dilution (not represented), which means that more general solvent properties than the simple dielectric constant have to be considered in the solvation process.

These subtle effects become very difficult to detect with anions of lower symmetry, such as TFSI⁻, which presents in addition an equilibrium between the *transoid* (C₂ symmetry) and *cisoid* (C₁ symmetry) conformers in the liquid state. The spectroscopic signature of the two TFSI⁻ conformers could be evidenced in a variety of systems,^[9–11,16] but we were not able to find any clear indication of ionic interaction effects on the TFSI⁻ spectra in bulk ILs involving this anion or even in the [EMI][TFSI] crystalline phases.^[16]

The cation vibrations

Although most 1,3-dialkylimidazolium cations are of low symmetry and present conformational isomerism, i.e. properties that hinder packing, favour the formation of ILs and simultaneously complicate the spectra analysis, they also hold three C–H oscillators that constitute potential spectroscopic probes for ion–ion interactions. Some authors even claim that the imidazolium C–H bonds, and particularly the more acidic C₍₂₎–H one, are involved in strong and directional hydrogen bonds with the IL anions.^[12,27–31,38–40] As this is a controversial issue still,^[25,43–44,60–65] and thus needs to be resolved, we have here focussed our analysis on the IR and Raman spectra of the C–H vibrations using H/D substitution effects.

Table 1. Observed anion vibrations for [BMI][PF₆] at room temperature

Symmetry	ν_1	ν_2	ν_3	ν_4	ν_5	ν_6
O _h	A _{1g} (R)	E _g (R)	F _{1u} (IR)	F _{1u} (IR)	F _{2g} (R)	F _{2u}
C _{4v}	A ₁ (IR, R)	A ₁ (IR, R); B ₁ (R)	A ₁ (IR, R); E(IR, R)	A ₁ (IR, R); E(IR, R)	B ₂ (R); E(IR, R)	B ₁ (R); E(IR, R)
IR (cm ⁻¹)	741 ^a		841	557.5	470 ^a	–
Raman (cm ⁻¹)	741	567	864 ^a	560 ^a	470	

^a Vibrations normally IR or Raman inactive in the O_h symmetry.

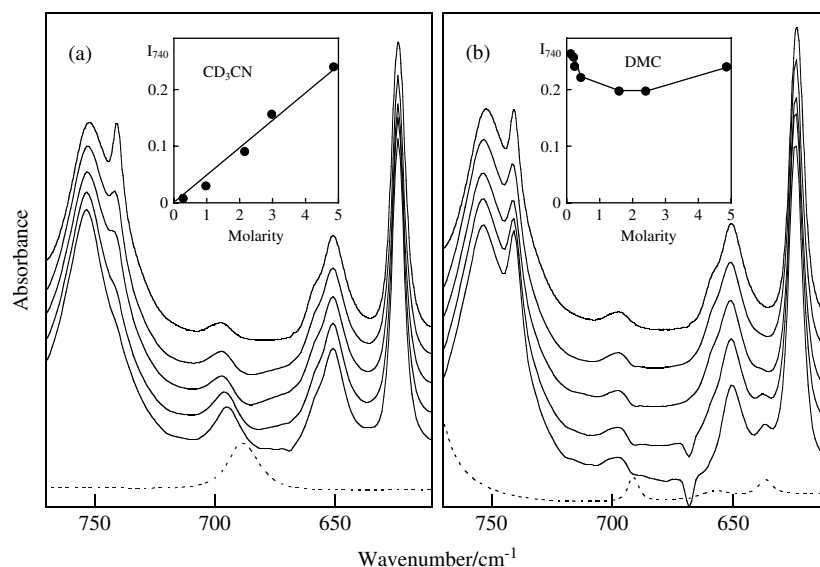


Figure 1. IR spectra of [BMI][PF₆] solutions in (a) CD₃CN and (b) DMC. Solid lines from top to bottom: pure [BMI][PF₆] and 1/2.5, 1/5, 1/25, 1/100 solutions after subtraction of the solvent contribution (dotted line) and normalisation using the BMI⁺ band at 624 cm⁻¹ as a reference. The spectra are shifted along the ordinate axis for convenience. The 670 cm⁻¹ dip comes from the (ill-compensated) ν₂ deformation mode of atmospheric CO₂. In the inserts, the intensity of the ν₁ IR absorption of PF₆⁻ (*I*₇₄₀) normalised to the 624 cm⁻¹ BMI⁺ reference band is reported as a function of the [BMI][PF₆] concentration in either DMC or CD₃CN.

Selective deuteration of 1,3-dialkylimidazolium cations

The deuteration rates are classically followed by NMR,^[4,45–50,66,67] but they can also be conveniently controlled in the 1050–940 cm⁻¹ Raman region where the D₂O vibrations do not interfere significantly (Fig. 2). A cation band at 961 cm⁻¹, assigned below to the stretching vibration νC–C of the ethyl group, is practically unchanged by deuteration of the imidazolium CH bonds, while a band at 1025 cm⁻¹ in EMI-*d*₀ is shifts to 1016 cm⁻¹ in EMI-*d*₁ and to 1005 cm⁻¹ in EMI-*d*₃. Therefore, using the 961 cm⁻¹ band as an internal reference, the H/D exchange can be measured from the relative intensities of the 1025, 1016 and 1005 cm⁻¹ bands. The intensity decrease of the 1025 and 1016 cm⁻¹ bands as a function of minutes and days, respectively, is illustrated in the inserts of Fig. 2. We have not tried to determine accurately the deuteration kinetics, but only verified the degree of deuteration. Deuterium contents of more than 98% are obtained for the EMI-*d*₁ and EMI-*d*₃ derivatives. Interestingly, these qualitative observations convey some information on ion–ion interactions and solvation effects. First, without any added catalyst, the deuteration of the C₍₂₎H proton at room temperature is orders of magnitude faster than the deuteration of the C₍₄₎H and C₍₅₎H protons at 373 K. Second, the rate of the C₍₂₎H/C₍₂₎D exchange is strongly dependent on the EMI⁺ concentration in D₂O. It occurs on a time scale of about 1 h for a diluted solution (Fig. 2), but it is considerably slowed down for solutions more concentrated than [EMI⁺]/[D₂O] ~ 1/10. We believe that in dilute solutions the C₍₂₎H groups of the EMI⁺ cations are fully solvated by D₂O, while in concentrated solutions the number of IPs and clusters increases, shielding the C₍₂₎H group and making the H/D exchange more difficult. Third, the C₍₂₎H/C₍₂₎D exchange has an exponential behaviour, which is characteristic of a simple pseudo-first-order reaction. The data for the C_(2,4,5)H/C_(2,4,5)D exchange are less accurate and the intensity at 1016 cm⁻¹ does not go to zero because the 1005 cm⁻¹ band of the *d*₃ derivative is asymmetric and keeps a residual intensity at 1016 cm⁻¹. The absence of any detectable νCH band in the IR and Raman spectra of this *d*₃ derivative confirms that the H/D exchange

is above 98%. Giernoth and Bankman^[46,47] have determined more detailed reaction profiles by NMR. Yasaka *et al.*^[66] have made similar observations on D₂O solutions of [BMI][Cl] and given more sophisticated explanations in terms of water solvation and dynamics.

A practical conclusion can be drawn from the above studies: as already well established in the literature,^[4,45–47] the deuteration of the C₍₂₎H bond in 1,3-dialkylimidazolium derivatives associated with halide ions is found to be easy and rapid in D₂O solutions. Jeon *et al.*^[20] have exploited this property to investigate the IR spectrum of the [BMI-*d*₁][I] derivative after removal of the D₂O solvent, but other spectroscopic studies of [BMI][Cl]/D₂O and [BMI][Br]/D₂O solutions do not seem to have taken the H/D exchange into account although it occurs in the typical duration of an experiment.^[40]

In the case of the [EMI][TFSI] derivatives, the deuteration rates can be followed by the same method, as the 1050–940 cm⁻¹ Raman region is free from TFSI⁻ bands. This is illustrated in Fig. 3 after evaporation of the CD₃OD solvent under vacuum.

Characteristic vibrations of the cation below 1600 cm⁻¹

We have concentrated our analysis on the 1300–500 cm⁻¹ region which contains the in-plane (δCH and δCD) and out-of-plane (γCH and γCD) bending modes of the imidazolium cations. A monoatomic anion, Br⁻, has been chosen to allow all the vibrations of the cation to be investigated without any interference from anion contributions. Furthermore, since our main concern is to know how inter-ionic interactions affect the vibrational spectra, [EMI][Br] has been studied in dilute aqueous solution in the liquid state at 353 K and in the solid state at room temperature. The spectra of the solutions and of the crystal are proposed to assist our interpretation of the more complex liquid state. Finally, in the case of the MMI⁺ and EMI⁺ deuterated derivatives, the calculations of the harmonic and anharmonic wavenumbers of the isolated cations have been complemented by a determination

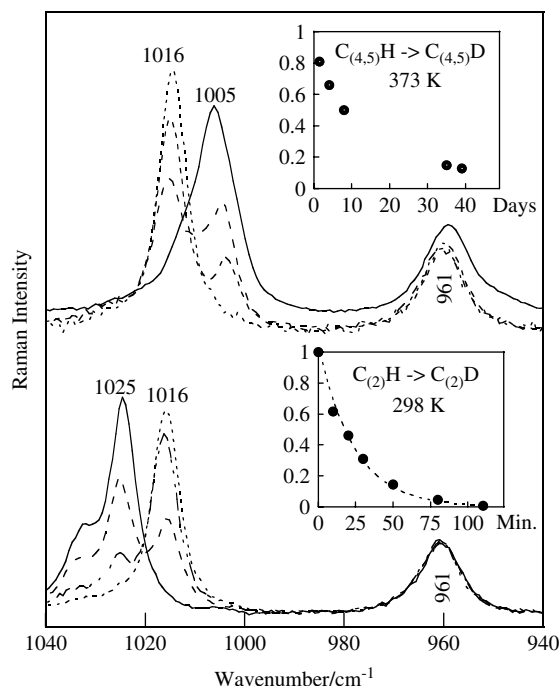


Figure 2. Raman spectra of a [EMI][Br]/D₂O = 1/30 solution as a function of time at 298 K (bottom) and at 373 K (top), using the 961 cm⁻¹ band as internal reference. The 1025, 1016 and 1005 cm⁻¹ bands are characteristic of the EMI-*d*₀, EMI-*d*₁ and EMI-*d*₃ derivatives, respectively. The decrease of the 1025 cm⁻¹ line (bottom) is reported at *t* = 0 and after 10, 30 and 120 min. The decrease of the 1016 cm⁻¹ line (top) is reported at *t* = 0 and after 37, 160 and 840 h. The corresponding deuteration rates are illustrated in the inserts.

of the PED of the normal modes involved for each IR or Raman transition.

The aqueous solutions of the four isotopic derivatives of [EMI][Br] are first considered. If the dilution is large enough to produce SSIPs, the experimental spectra should be directly comparable to those calculated for isolated cations. It is then interesting to consider the [EMI][Br] crystal of known structure (*P*2₁/*C*, *Z* = 4) where the cations are localised in a well-defined and rigid geometrical environment.^[68] The ethyl group is situated out of the ring plane (non-planar conformation). Each cation has three neighbouring anions with a C₍₂₎···Br⁻ distance of 0.3575 nm and C₍₄₎···Br⁻ and C₍₅₎···Br⁻ distances of 0.3820 nm. A first inspection of Fig. 4 shows that the calculated anharmonic wavenumbers for the four isotopic derivatives reproduce well the experimental spectra with a multiplicative scaling factor of only 1.01 (the harmonic wavenumbers would give a comparable agreement if multiplied by 0.989). A number of lines are relatively constant in position and width in the three physical states, e.g. the ν_{CC} line of the ethyl group at 961 cm⁻¹ and the ν_{ip}N-CH₃ line at 600 cm⁻¹.

The analysis of the PEDs of MMI-*d*₀ of C_{2v} symmetry and EMI-*d*₀ of pseudo-C_{2v} symmetry (Tables S1 and S3) reveals that the δC_{(2)H} and δ_{op}C_{(4,5)H} vibrations of B₂ symmetry in C_{2v} are mixed together and with other modes, in particular the twisting of the methylene group (tCH₂) in the case of EMI-*d*₀, to give three lines calculated/observed at 1291/1299, 1242/1251 and 1153/1173 cm⁻¹, while the δ_{ip}C_{(4,5)H} vibration (70%) of A₁ symmetry in C_{2v} is found at 1115/1115 cm⁻¹ (Fig. 4). Deuteration of the C_{(2)H} bond in EMI-*d*₁ simplifies the situation. The δ_{op}C_{(4,5)H} mode is still mixed with tCH₂ to give the lines calculated/observed at 1271/1280 and 1222/1229 cm⁻¹, but δ_{ip}C_{(4,5)H} (80%) appears at 1114/1112 cm⁻¹ and δC_{(2)D} (65%) at

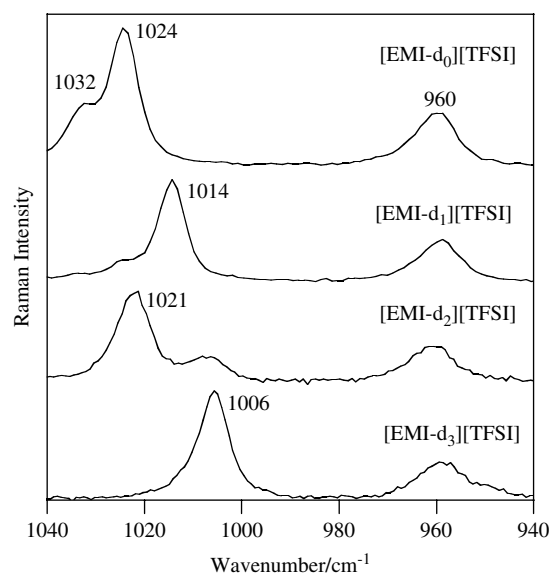


Figure 3. Raman spectra of the [EMI][TFSI] deuterated derivatives at room temperature in a region of transparency of the anion.

892/898 cm⁻¹ (Tables S2 and S4). The δC_{(2)D} line is much broader in the solution and liquid states than in the solid. It constitutes an ideal spectroscopic probe, as it is little perturbed by coupling or mixing with other modes. However, its sensitivity to ionic interactions is weak, as indicated by a constant position at ~898 cm⁻¹ in the three states. In the EMI-*d*₂ derivative, the δC_{(2)H}, δ_{op}C_{(4,5)D} and δ_{ip}C_{(4,5)D} modes give isolated lines calculated/observed at 1200/1210, 901/903 and 807/805 cm⁻¹ in solution, respectively (Table S5). They are slightly shifted to 1211, 908 and 813 cm⁻¹ in the solid, respectively (Fig. 4). Finally, in the EMI-*d*₃ derivative (Fig. 4), a mixing occurs again between δC_{(2)D}, δ_{op}C_{(4,5)D} and other modes, while the δ_{ip}C_{(4,5)D} is well isolated at 807/801 cm⁻¹ and shifted to 811 cm⁻¹ in the solid (Table S6).

The same approach is used for the assignment of the γCH/D modes. In EMI-*d*₀, a mixing occurs now between the γC_{(2)H} and γ_{ip}C_{(4,5)H} modes, of B₁ symmetry in C_{2v}, while the γ_{op}C_{(4,5)H} mode is better localised. This γ_{op}C_{(4,5)H} mode, of A₂ symmetry in C_{2v}, has, however, zero intensity in IR and Raman and the former two have a weak Raman activity but a strong IR intensity. These theoretical predictions are expected to be somewhat relaxed by the pseudo-C_{2v} symmetry of EMI-*d*₀ and by the anharmonic character of these vibrations. It is already obvious from Fig. 4 that strong differences occur between the solution and the solid state. In the solid state, four well-defined lines appear at 889, 871, 806 and 789 cm⁻¹. The weak 806 cm⁻¹ band comes from a rocking of the CH₂ group, but the other three lines have a γCH character, although they are calculated at lower wavenumbers and with very weak Raman intensities. As they give broad profiles in the liquid and vanish in solution, one can infer that they are activated in the solid phase by the C-H···Br⁻ interactions and by their anharmonic character. The simple deuteration of the C_{(2)H} bond in EMI-*d*₁ brings strong changes to this region. The PED of EMI-*d*₁ show that the γC_{(2)D} mode is now mixed with a large number of out-of-plane ring modes and participates to the transitions calculated at 704 and 534 cm⁻¹. The latter is observed at 558 cm⁻¹ in the solid, but the former is more difficult to identify because of the presence of a strong line mainly due to the γ_{ip}C_{(4,5)H} vibration at 732 cm⁻¹. All these lines become again broad and weak in the liquid and

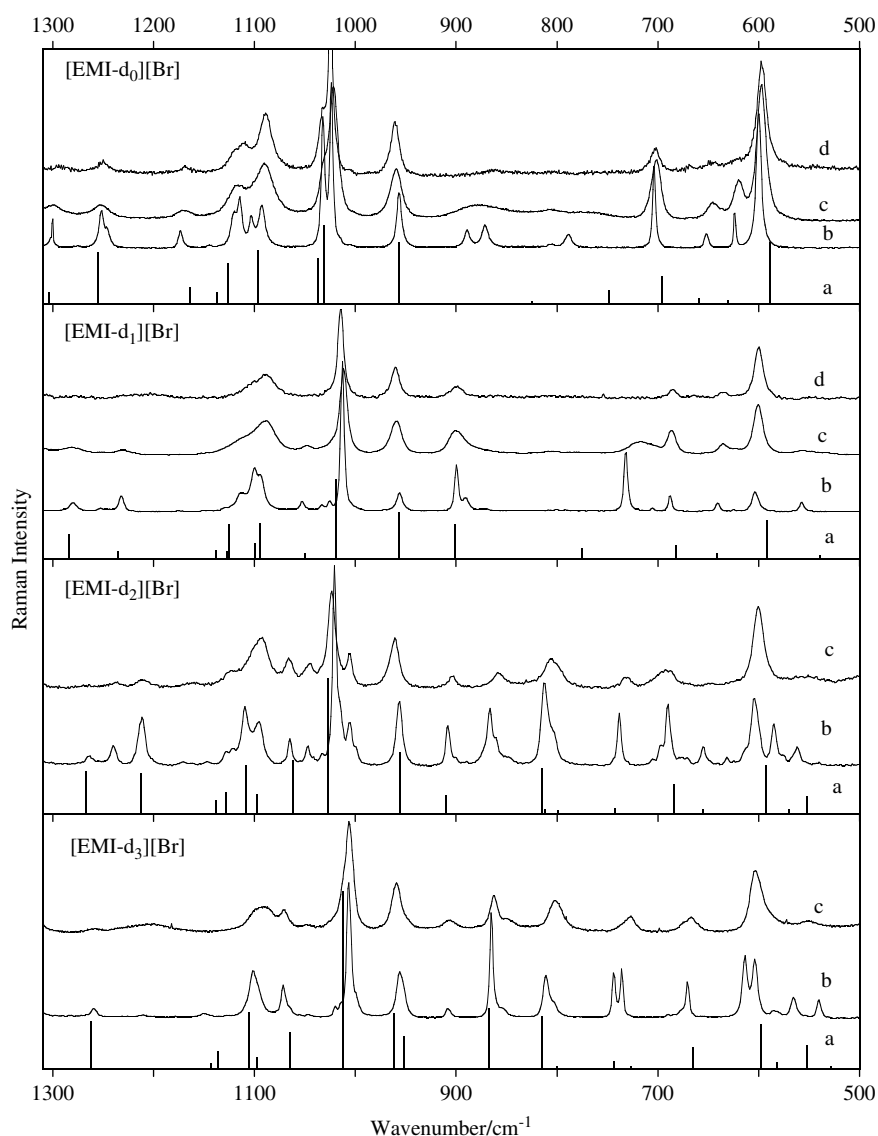


Figure 4. Raman spectra of the four indicated [EMI][Br] derivatives. Comparison of the calculated anharmonic Raman spectra (a) with the experimental Raman spectra of solid [EMI][Br] at 298 K (b), liquid [EMI][Br] at 353 K (c) and a 1/30 [EMI][Br]/H₂O solution (d). The calculated wavenumbers are multiplied by a scaling factor of 1.01.

vanish in solution. For the EMI-*d*₂ derivative, the $\gamma_{C(2)H}$ vibration calculated at 804 cm⁻¹ (67%) gives a line at 858 cm⁻¹ in solution and shifted to 866 cm⁻¹ in the solid. The $\gamma_{opC(4,5)D}$ and $\gamma_{ipC(4,5)D}$ vibrations produce the lines calculated/observed at 735/738 and 564/585 cm⁻¹, respectively. In EMI-*d*₃, the $\gamma_{C(2)D}$ is again mixed with several out-of-plane ring modes to give two components calculated/observed at 720/735 and 524/541 cm⁻¹. The $\gamma_{opC(4,5)D}$ and $\gamma_{ipC(4,5)D}$ vibrations give the 736/744 and 576/584 cm⁻¹ lines, respectively.

These tedious but indispensable assignments confirm that the $\gamma_{CH/D}$ vibrations are more sensitive than the $\delta_{CH/D}$ ones to inter-ionic interactions, but they are also more complicated because of their mixing with several out-of-plane ring modes. If an internal mode of the cation insensitive to the deuteration, such as the ν_{CC} Raman line at 961 cm⁻¹, is taken again as a reference, it appears that the γ_{CH} lines have about the same width as the reference line in the solid state, but they become three to four times broader in the liquid state and often vanish in solution, in agreement

with the very weak calculated Raman intensities for an isolated cation. The γ_{CH} vibrations have a much stronger IR activity as illustrated in Fig. 5 for liquid [EMI][Br]. In between the two modes at 961 cm⁻¹ (ν_{CC}) and 700 cm⁻¹ (ν_{opNCH_2}), present in both IR and Raman spectra, the IR spectrum exhibits two broad and intense absorptions at 820 and 749 cm⁻¹ which can be assigned to the $\gamma_{C(2)H}$ and $\gamma_{ipC(4,5)H}$ vibrations, respectively, in agreement with the strong intensities calculated at 816 and 741 cm⁻¹. Once this assignment is established, it becomes possible to compare the IR spectra of various ILs (Fig. 6). The 750 cm⁻¹ $\gamma_{ipC(4,5)H}$ band is hardly sensitive to the nature of the anion. On the other hand, the profile and position of the band at 800–850 cm⁻¹, mainly due to $\gamma_{C(2)H}$, change noticeably. As expected, it disappears in [BMMI][TFSI] when the C_{(2)H} bond is methylated, which is a further argument for its assignment, but in the other derivatives its mean position shifts to low wavenumbers and becomes asymmetric when the anion becomes more basic. Increasing ion–ion interactions are expected to produce a blue shift of $\gamma_{C(2)H}$. Therefore, the observed red shift

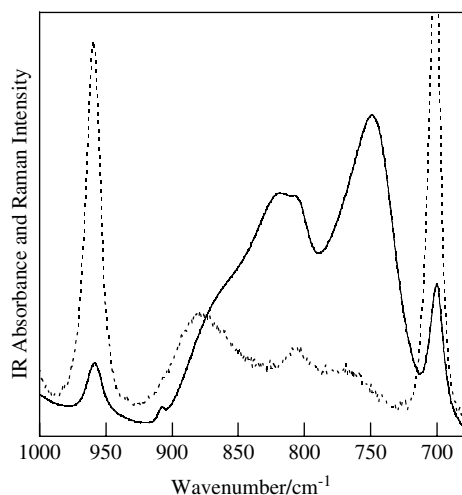


Figure 5. Comparison of the IR (solid line) and Raman (dotted line) spectra of liquid [EMI][Br] at 353 K in the region of the γ CH vibrations.

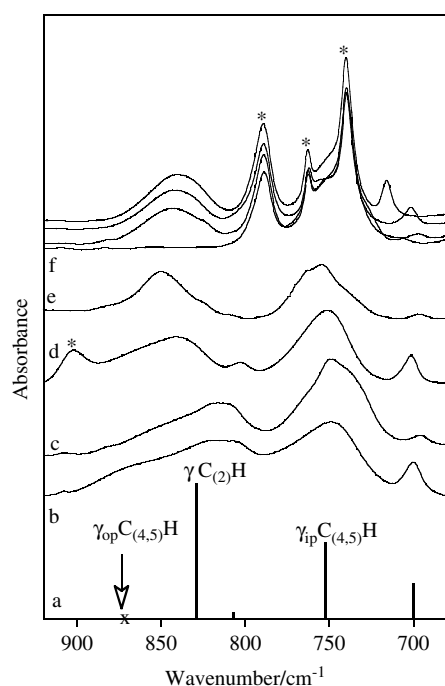


Figure 6. Comparison of (a) the calculated anharmonic IR spectra of EMI- d_0 with a multiplicative scaling factor of 1.015 and the experimental IR spectra of (b) [EMI][Br], (c) [EMI][I], (d) [EMI][N(CN) $_2$], (e) [EMI][BF $_4$] and (f) [C][TFSI] with C = BMMI, BMI, EMI and MMI from bottom to top. All spectra were recorded at room temperature except (b) and (c), which were at 353 K. Asterisks indicate internal modes of the N(CN) $_2^-$ or TFSI $^-$ anions.

is mainly due to changes in the vibrational couplings. A modest but normal blue shift is observed for the γ C $_{(2)}$ D low-wavenumber component in various EMI- d_1 derivatives. Indeed, when the anion is varied in the series FSI $^-$, N(CN) $_2^-$, SCN $^-$, Br $^-$, this vibration shifts from 540 to 544, 546 and 556 cm $^{-1}$, respectively.

In the comparison between the experimental and calculated spectra, we have only used the calculated spectra of the non-planar form of EMI $^+$ because it is of lower energy than the planar form and its contribution is predominant at room temperature. The calculation indicates that the conformational splittings are

generally too small to be resolved, except in the 400–200 cm $^{-1}$ region of the Raman spectra where the conformational equilibrium can indeed be investigated.^[8,16]

Characteristic vibrations of the cation above 2800 cm $^{-1}$

A clear distinction can be made between the ν CH $_2$ and ν CH $_3$ stretching vibrations of the substituted alkyl groups occurring in the 2800–3000 cm $^{-1}$ region and the ν CH stretching vibrations of the imidazolium CH groups situated between 3000 and 3200 cm $^{-1}$. Furthermore, it is now well established that the IR spectra of ILs involving weakly coordinating anions exhibit two main ν CH absorptions at 3160 \pm 15 and 3120 \pm 15 cm $^{-1}$.^[42] The first absorption has often been assigned to the ν_{ip} C $_{(4,5)}$ H and ν_{op} C $_{(4,5)}$ H vibrations (where ip and op mean in-phase and out-of-phase, respectively) and the second to the ν C $_{(2)}$ H vibration shifted by C $_{(2)}$ H \cdots anion hydrogen bond interactions. Ludwig *et al.* even distinguish in the second absorption C $_{(2)}$ H oscillators involved in aggregates at \sim 3125 cm $^{-1}$ and in IPs at \sim 3105 cm $^{-1}$.^[12] Umabayashi *et al.*^[41] observe that the 3102 cm $^{-1}$ shoulder becomes relatively intense when [EMI][TFSI] is dissolved in CD $_3$ CN and they conclude that it corresponds to an isolated (dissociated) structure in equilibrium with an associated structure characterised by the 3125 cm $^{-1}$ component. The two above interpretations can be reconciled if isolated (dissociated) structure means IPs and associated structure means larger ion clusters. However, the existence of two kinds of C $_{(2)}$ H groups is not corroborated by the C $_{(2)}$ H/C $_{(2)}$ D isotopic exchange.^[42] Indeed, a simple ν C $_{(2)}$ D absorption band is reported for [EMI- d_1][AlCl $_4$],^[4] [EMI- d_1][TFSI],^[42] [EMI- d_1][BF $_4$],^[14] [BMI- d_1][I],^[20] and [EMI- d_1][C].^[4] at 2350, 2350, 2358, 2300 and 2280 cm $^{-1}$, respectively. The observed red shift is in agreement with increasing anion basicity. In these monodeuterated derivatives, the ν CH region should become simpler, as it involves only the ν_{op} C $_{(4,5)}$ H and ν_{ip} C $_{(4,5)}$ H vibrations. However, more than two components are generally observed and different assignments are proposed. It must also be pointed out that the only examples in the literature of fully deuterated compounds, [EMI- d_3][AlCl $_4$]^[4] and [EMI- d_3][TFSI],^[42] indicate that the IR band shape of the ν CD vibrations is very different from the ν CH band shape composed of two main absorptions.

For a better understanding of the complex ν CH region, we recently proposed a completely new approach where the intrinsic anharmonicity of the CH oscillators and of their couplings by Fermi resonances with overtones and combination of the in-plane R $_1$ and R $_2$ ring modes were taken into account.^[42] This study was limited to the IR spectra of ILs involving weakly coordinating anions such as PF $_6^-$, BF $_4^-$ or TFSI $^-$, but it takes advantage of selective H/D isotopic exchanges on the imidazolium moiety. The proposed new assignment is controversial, as any interpretation of the ν CH region in terms of CH \cdots anion H-bond interactions seems to become obsolete.^[25,42,43] Therefore, we here revisit and extend our analysis by using the complementary Raman spectra and more basic anions.

Let us first consider the Raman spectra of the [EMI][TFSI] isotopic derivatives (Fig. 7). They are presented in the same form as the IR spectra (Fig. S1, Supporting Information) to facilitate comparison. The PEDs show that the three ν CH modes are not 'degenerated', as sometimes stated in the literature, but vibrate independently (Tables S1–6). As usual, the modes of symmetry close to A $_1$ have a predominant Raman intensity. Thus, the ν_{ip} C $_{(4,5)}$ H/D lines are more intense than the ν_{op} C $_{(4,5)}$ H/D ones and the R $_1$ transition is more intense than R $_2$, as opposed to what happens in IR. Nevertheless,

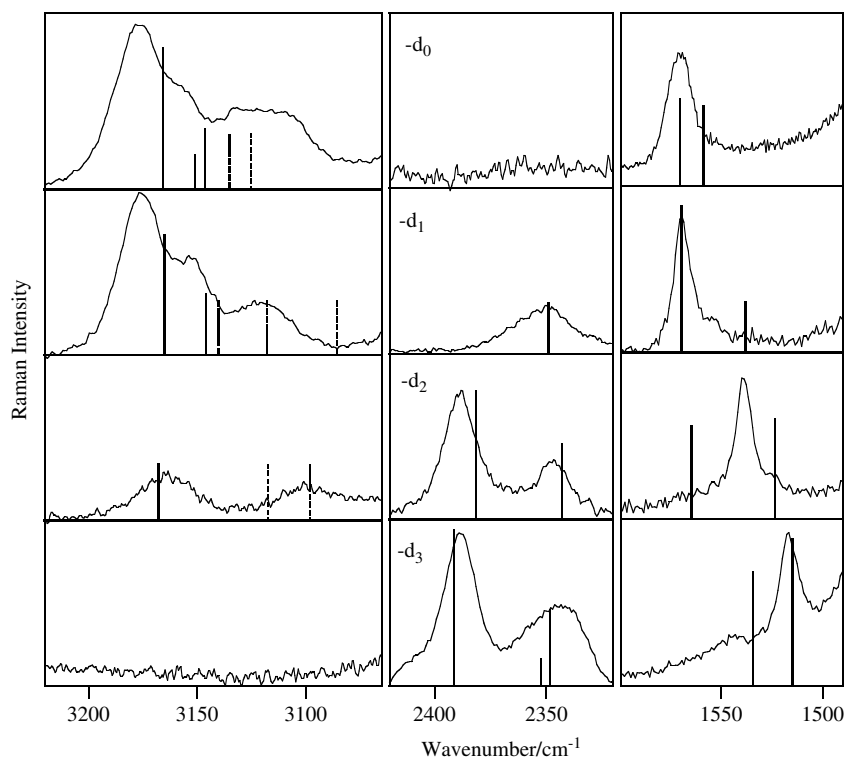


Figure 7. Raman spectra of the [EMI][TFSI] deuterated derivatives in the region of the ν_{CH} stretching vibrations (left), ν_{CD} stretching vibrations (middle) and in-plane ring modes R_1 and R_2 (right). The calculated anharmonic wavenumbers (vertical solid lines) have been multiplied by a scaling factor of 0.9939 for the left and middle spectra and of 0.9949 for the right spectra. The vertical dotted lines correspond to the overtones and combination of the R_1 and R_2 modes.^[42] They are given arbitrary intensities.

all the arguments developed to assign the IR spectra can be reused. The more striking observation concerns the $\nu_{\text{C}(2)\text{D}}$ vibration in EMI- d_1 , which gives only one band at $\sim 2351\text{ cm}^{-1}$, whereas the $\nu_{\text{C}(2)\text{H}}$ vibration in EMI- d_2 gives two bands of similar intensity at 3164 and 3100 cm^{-1} , which are interpreted by a Fermi resonance between the $\nu_{\text{C}(2)\text{H}}$ mode and the $2R_1$ overtone. A very strong coupling is indeed theoretically predicted between these two levels.^[42] It means that both the 3164 and 3100 cm^{-1} bands have a $\nu_{\text{C}(2)\text{H}}$ character. The unperturbed $\nu_{\text{C}(2)\text{H}}$ vibration must be situated in between, at about 3132 cm^{-1} , giving a $\nu_{\text{C}(2)\text{H}}/\nu_{\text{C}(2)\text{D}}$ isotopic ratio of 1.33. The results obtained for the $\nu_{\text{C}(2)\text{D}}$ vibration, including those in the literature on other [EMI- d_1] derivatives,^[4,14,20,42] are easier to interpret, as the uncoupled $\nu_{\text{C}(2)\text{D}}$ vibration constitutes a direct spectroscopic probe of the interactions experienced by the [EMI- d_1]⁺ cation. On the other hand, the $\nu_{\text{C}(2)\text{H}}$ mode seems to be systematically complicated by Fermi resonances. It is remarkable that all the spectroscopic features of Fig. 7, except those for $\nu_{\text{C}(2)\text{H}}$, are well predicted by the calculated anharmonic wavenumbers and intensities (from the harmonic approximation).

As already observed with the in-plane δCH and out-of-plane γCH bending modes, the ion–ion interactions induce in the liquid phase a considerable broadening of the $\nu_{\text{CH/D}}$ transitions. Thus, the full-width at half-maximum of the $\nu_{\text{C}(2)\text{D}}$ and R_1 Raman bands in liquid [EMI- d_1][TFSI] are 34 and 8 cm^{-1} , respectively (Fig. 7). The $\nu_{\text{CH/D}}$ vibrations are very anharmonic and the fluctuations of their environment, and hence of their orientation relative to the anion, produce an inhomogeneous broadening.

The assignment of the $\nu_{\text{CH/D}}$ modes developed above for [EMI][TFSI] applies to other ILs involving weakly coordinating anions such as FSI⁻, BETI⁻, BF₄⁻, PF₆⁻, AlCl₄⁻ or B(CN)₄⁻, as

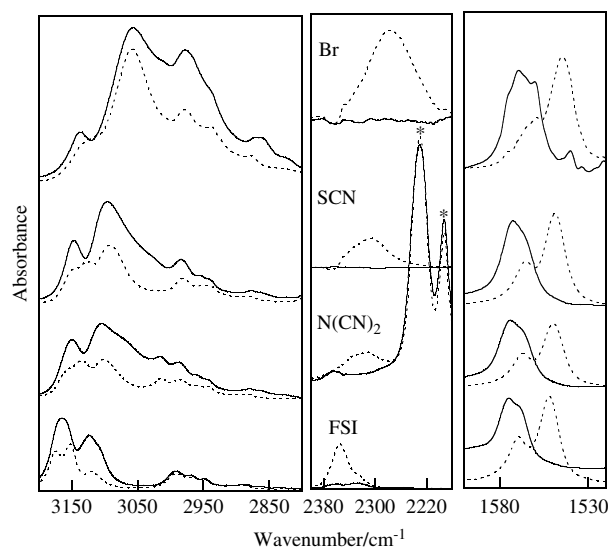


Figure 8. IR spectra of [EMI- d_0][X] (solid line) and [EMI- d_1][X] (dotted line) ILs (with X = FSI, N(CN)₂, SCN and Br) in the region of the ν_{CH} stretching vibrations (left), ν_{CD} stretching vibrations (middle) and in-plane R_1 and R_2 ring vibrations (right). All samples are at room temperature, except [EMI][Br] melted at 353 K. The asterisks indicate internal modes of the N(CN)₂ anion.

very similar IR and Raman profiles are observed for the whole series. However, these profiles change markedly with more basic anions, as illustrated in Fig. 8 for the IR spectra of [EMI- d_0][X] and [EMI- d_1][X] ILs with X = FSI, N(CN)₂, SCN and Br, as already

pointed out by Wulf *et al.*^[43] On the other hand, the R_1 and R_2 ring modes are much less perturbed by the nature of the anion than by the H/D exchange. As previously commented, with increasing anion basicity the $\nu_{C(2)D}$ band shifts to lower wavenumbers and becomes broader and more intense. The behaviour of the ν_{CH} absorptions is again far more complex. The comparison of the profiles of the two isotopic derivatives shows intensity differences in a large wavenumber range. No straightforward identification of a $\nu_{C(2)H}$ band is possible. Note that for [EMI][Br] the two absorptions at 3137 cm^{-1} and 3062 cm^{-1} are present in the d_0 as well as in the d_1 derivative. Furthermore, the 2980 cm^{-1} band involves a contribution of the substituted methyl group. We have not been able to interpret clearly these ν_{CH} profiles, and we believe that it is very difficult to extract any information from this spectral region where the respective effects of Fermi resonances and of increasing $C-H\cdots$ anion interactions are mixed. The situation is even less favourable in the Raman spectra, where the intensity of the stretching vibrations of the alkyl groups becomes much more intense than those of the imidazolium CH groups. The ν_{CH} region is definitely too complex to provide unambiguous information on the $C-H\cdots$ anion interactions.

The $\nu_{C(2)D}$ vibrations of the monodeuterated cations are far more favourable because the $C(2)D$ bond is a quasi-diatomic oscillator, uncoupled to the other vibrations and free from Fermi-resonance perturbations. The $\nu_{C(2)D}$ vibration gives a well-isolated band at about $2355\text{--}2350\text{ cm}^{-1}$ for the weakly coordinating anions. It becomes broader and asymmetric with the more basic $N(CN)_2^-$, SCN^- , I^- and Br^- anions and shifts to 2314 , 2306 , 2300 and 2280 cm^{-1} , respectively. This red shift has to be associated with the blue shift previously described for $\gamma_{C(2)D}$. The two extreme cases of [EMI- d_1][TFSI] and [EMI- d_1][Br] are reported in Fig. 9. They illustrate the red shift and broadening occurring on the Raman $\nu_{C(2)D}$ band between the two ILs. The interactions between the CH imidazolium bonds and the bromide anions in crystalline [EMI][Br] phase have been described by Elaiwi *et al.*^[68] in terms of $C-H\cdots Br^-$ hydrogen bonds. It is tempting to interpret also the results of Fig. 9 by a $C(2)-D\cdots$ anion hydrogen bond, weak in the case of TFSI⁻ and stronger with Br^- . However, in melted [EMI- d_1][Br], the $\nu_{C(2)D}$ band is considerably broader than

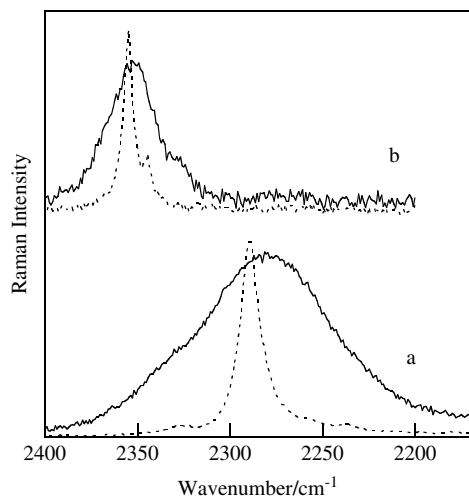


Figure 9. Raman spectra of the $\nu_{C(2)D}$ vibration in (a) [EMI- d_1][Br], liquid at 353 K (solid line) and solid at room temperature (dotted line), (b) [EMI- d_1][TFSI] liquid at room temperature (solid line) and solid at 110 K (dotted line).

in the crystal and its maximum is situated at 2280 cm^{-1} , compared to 2289 cm^{-1} , which is an unusual feature for a conventional hydrogen bond which is expected to be stronger in the crystal. One can infer that in the melt the bromide anions can occupy a variety of positions relative to the imidazolium ring and hence to the $C(2)-D$ bond. Not all these positions can satisfy the formation of directional $C(2)-D\cdots Br^-$ hydrogen bonds. Actually, a number of theoretical studies have explored the potential intermolecular energies of IPs formed between an imidazolium ring and a variety of anions, including halides.^[25,60–65] There is a clear tendency to consider that the orientation of the anion relative to the $C(2)-H$ bond does not greatly affect the size of the interaction energy.^[60–65] Because of this lack of directionality, the term of unconventional hydrogen bond has been introduced and this unconventional character might well be reflected by the position and width of the $\nu_{C(2)-D}$ band for the liquid samples in Fig. 9.

Intermolecular cation–anion vibrations

A more direct insight into the ion–ion interactions in ILs is provided by the far-IR region. It has already been demonstrated that below about 200 cm^{-1} there are few intramolecular vibrations of the cations and anions and, in addition, their IR intensities are much weaker than the broad absorption centred at $100 \pm 20\text{ cm}^{-1}$ due to intermolecular cation–anion vibrations.^[26–33] According to Ludwig *et al.*, the intermolecular vibrations that give the main contribution to the far-IR absorption are the stretching and bending modes of the $C(2)-H\cdots$ anion hydrogen bond.^[31] We have recently shown that this interpretation is not corroborated by ILs that do not involve the acidic $C(2)-H$ imidazolium bond.^[32] Indeed, as illustrated again in Fig. 10 by a comparison of various TFSI-based ILs, a far-IR absorption of comparable intensity is observed around 80 cm^{-1} even when the $C(2)H$ group of BMI is methylated in BMMI or when the cation holds very weakly acidic protons as in tetra-alkyl ammonium or pyrrolidinium. It must be pointed out that the intramolecular vibrations of the TFSI⁻ anion

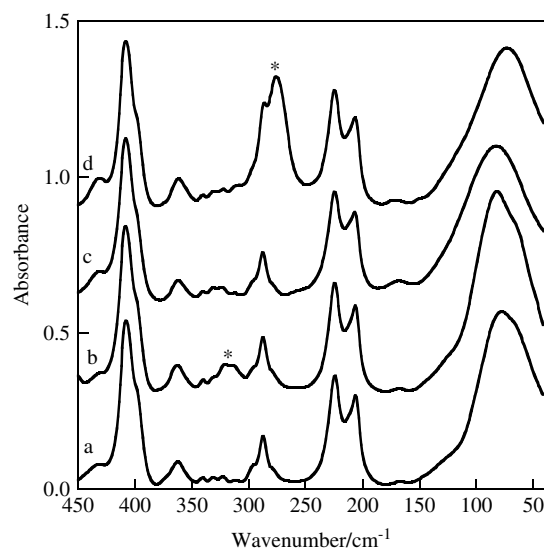


Figure 10. Far-IR spectra of (a) [BuMePyr][TFSI], (b) [Me₃BuN][TFSI], (c) [BMI][TFSI] and (d) [BMMI][TFSI] at room temperature with a thickness of $50\text{ }\mu\text{m}$. The anion bands above 200 cm^{-1} have been brought to similar intensities for a qualitative normalisation. Asterisks indicate absorptions due to the internal modes of the cations. The spectra are shifted by 0.3 absorbance units for convenience.

situated at 206, 224 and 408 cm^{-1} are practically insensitive to the cation–anion interactions and can be used as internal references in the comparison. To describe the intermolecular vibrations responsible for the far-IR absorption, it is necessary to consider a model of local structure for the cation–anion interactions. In agreement with Ludwig *et al.*,^[29–31] we found that the calculated spectra of (cation–anion)_n ion-pair dimers ($n = 2$) give a better agreement with the observed absorption band than simple IPs ($n = 1$).^[32] However, larger clusters ($n > 2$) give a comparable agreement to ion-pair dimers and it is not possible to decide which is the optimal n value or whether there is an equilibrium between clusters of different sizes.^[69,70] In any case, the far-IR absorption is composed of a series of transitions corresponding to translational (rattling) and rotational (librations) motions of the cations and anions inside their respective solvation cages. They can be viewed as a vibrational density of states and they occur for any cation–anion combination, independently of the presence of proton donor groups on the cation.

It follows from the above discussion that progress in the improvement of the vibrational assignments needs more realistic models of the local structure in ILs (and vice versa). This is true for the far-IR absorption, but applies also to the interpretation of the intramolecular vibrations and more specifically to the complex νCH vibrations.

Conclusion

A more complete picture of the origins of the detailed features in the IR and Raman spectra of ILs has emerged by using complementary information and checking for internal consistency, in various spectral regions and for anion, cation and intermolecular vibrations. In ILs involving anions of high symmetry, such as PF_6^- , unexpected IR and Raman activities are observed although the characteristic wavenumbers are those of a ‘free’ anion. This is qualitatively interpreted in terms of an anion submitted to a weakly anisotropic electrostatic field. Indeed, when the IL is dissolved in polar solvents to form SSIPs, the selection rules of an octahedron are obeyed. On the other hand, the anion seems to form IPs in non-polar solvents with an increased IR intensity, e.g. the symmetric stretching mode of the PF_6^- anion. As far as we know, this classical approach of ion-pairing effects in alkali-metal solutions^[58,59] has never been applied to ILs. Although the spectroscopic effects are weak and limited to intensities, they may provide a new insight into ion–ion interactions in ILs. They have anyway to be reproduced by any model of local structure. The terms polar and non-polar solvents, or the simple consideration of the solvent dielectric constant, are also clearly insufficient to describe the solvation processes. Further studies with a variety of solvents and ILs are needed for a more detailed modelling.

The vibrational assignment of the imidazolium cations proves to be very difficult in spite of the help of isotopic derivatives and of DFT calculations. Below 1600 cm^{-1} , this is due to a mixing of the in-plane and out-of-plane deformations of the CH groups with ring vibrations of the same symmetry. Above 3000 cm^{-1} , the three stretching vibrations of the CH groups are well separated from any other internal vibration. Furthermore, their PEDs, calculated in the harmonic approximation (Tables S1–6), are close to 100%, showing that they constitute three independent group vibrations. However, these νCH vibrations are intrinsically very anharmonic and they undergo anharmonic couplings by Fermi resonance with the overtones and combination of two in-plane ring modes. As a

consequence, it becomes extremely difficult to disentangle purely spectroscopic effects from spectral perturbations due to ion–ion interactions. The variations of the νCH profile in ILs as a function of the nature of the anion, temperature, pressure or any other parameter have to be interpreted with great care. In the liquid state, these vibrations are affected both by Fermi resonance and by a strong inhomogeneous broadening due to the strength and variation of the ion–ion interactions. There is only one situation where the vibrational analysis simplifies: the pseudo-diatom $\text{C}_{(2)}\text{D}$ oscillator in EMI-d_1 seems to be free from any Fermi resonance interaction and it occurs in a transparent spectral range. As monodeuterated imidazolium derivatives are easy to synthesise, the $\nu\text{C}_{(2)}\text{D}$ vibration appears to be the best candidate to study the ion–ion interactions in ILs, although it still gives broad and slightly asymmetric bands. The red shift, broadening and intensification of $\nu\text{C}_{(2)}\text{D}$ when going from weakly coordinating anions to, e.g., Br^- , are typical of increasing hydrogen-bond interactions. However, there are still controversies to know whether the $\text{C-H}\cdots\text{anion}$ interactions are conventional hydrogen bonds. The question is partially solved by a systematic investigation of the far-IR absorption occurring at $80 \pm 20 \text{ cm}^{-1}$. Indeed, this absorption, previously interpreted in terms of hydrogen bonding, is here shown to appear very similar even for ILs with cations unable to establish any hydrogen bonds, and the absorption is thus better interpreted in terms of electrostatic interactions between cations and anions. The imidazolium cation is highly polarisable and its interaction with anions of variable coordinating power induces a very specific reorganisation of the electron density, depending on the cation–anion orientation, as shown, e.g., by Hunt *et al.*^[64] Although everybody agrees that long-range Coulombic interactions are dominant, the local contribution of donor–acceptor interactions in the Lewis sense has certainly a much more general impact than those in the Brønsted sense (hydrogen bond). Charge-transfer complexes have recently been evidenced in the $[\text{BMI}][\text{I}]$ system by Katoh *et al.*^[62] Although iodide is a particularly good electron donor, charge transfer might well occur also with other anions and contribute to the local structuration in ILs and possibly to the spectroscopic response of ILs via the electronic structure.

Acknowledgements

The authors are grateful to C. Aupetit, J.-L. Bruneel and D. Talaga for their help in recording the IR and Raman spectra. Financial support from Stiftelsen J. Gust. Richert and the Swedish Research Council (VR) is gratefully acknowledged as well as the computational grant from SNAC to the C^3SE and NSC resources.

Supporting information

Supporting information may be found in the online version of this article.

References

- [1] M. Armand, F. Endres, D. R. MacFarlane, H. Ohno, B. Scrosati, *Nat. Mater.* **2009**, *8*, 621.
- [2] F. Endres, *Phys. Chem. Chem. Phys.* **2010**, *12*, 1648.
- [3] P. Bonhôte, A. P. Dias, N. Papageorgiou, K. Kalyanasundaram, M. Grätzel, *Inorg. Chem.* **1996**, *35*, 1168.
- [4] K. M. Dieter, C. J. Dymek, N. E. Heimer, J. W. Rovang, J. S. Wilkes, *J. Am. Chem. Soc.* **1998**, *110*, 2722.
- [5] S. A. Katsyuba, P. J. Dyson, E. E. Vandyukova, A. V. Chernova, A. Vidiš, *Helv. Chim. Acta* **2004**, *87*, 2556.

- [6] J. D. Holbrey, W. M. Reichert, R. D. Rogers, *Dalton Trans.* **2004**, 2267.
- [7] E. R. Talaty, S. Raja, V. J. Storhaug, A. Dolle, W. R. Carper, *J. Phys. Chem. B* **2004**, *108*, 13177.
- [8] Y. Umebayashi, T. Fujimori, T. Sukizaki, M. Asada, K. Fujii, R. Kanzaki, S.-I. Ishiguro, *J. Phys. Chem. A* **2005**, *109*, 8976.
- [9] M. Herstedt, M. Smirnov, P. Johansson, M. Chami, J. Grondin, L. Servant, J.-C. Lassègues, *J. Raman Spectrosc.* **2005**, *36*, 762.
- [10] M. Herstedt, W. A. Henderson, M. Smirnov, L. Ducasse, L. Servant, D. Talaga, J.-C. Lassègues, *J. Mol. Struct.* **2006**, *783*, 145.
- [11] K. Fujii, T. Fujimori, T. Takamuku, R. Kanzaki, Y. Umebayashi, S.-I. Ishiguro, *J. Phys. Chem. B* **2006**, *110*, 8179.
- [12] T. Köddermann, C. Wertz, A. Heintz, R. Ludwig, *ChemPhysChem* **2006**, *7*, 1944.
- [13] J. Kiefer, J. Fries, A. Leipertz, *Appl. Spectrosc.* **2007**, *61*, 1306.
- [14] S. A. Katsyuba, E. E. Zvereva, A. Vidiš, P. J. Dyson, *J. Phys. Chem. A* **2007**, *111*, 352.
- [15] A. Yokozeki, D. J. Kasprzak, M. B. Shiflett, *Phys. Chem. Chem. Phys.* **2007**, *36*, 5018.
- [16] J.-C. Lassègues, J. Grondin, R. Holomb, P. Johansson, *J. Raman Spectrosc.* **2007**, *38*, 551.
- [17] R. Holomb, A. Martinelli, I. Albinsson, J.-C. Lassègues, P. Johansson, P. Jacobsson, *J. Raman Spectrosc.* **2008**, *39*, 793.
- [18] J. Scheers, P. Johansson, P. Jacobsson, *J. Electrochem. Soc.* **2008**, *155*, A628.
- [19] Y. Jeon, J. Sung, D. Kim, C. Seo, H. Cheong, Y. Ouchi, R. Ozawa, H.-O. Hamaguchi, *J. Phys. Chem. B* **2008**, *112*, 923.
- [20] Y. Jeon, J. Sung, C. Seo, H. Lim, H. Cheong, M. Kang, B. Moon, Y. Ouchi, D. Kim, *J. Phys. Chem. B* **2008**, *112*, 4735.
- [21] S. A. Katsyuba, T. P. Griažnova, A. Vidiš, P. J. Dyson, *J. Phys. Chem. B* **2009**, *113*, 5046.
- [22] Y. U. Paulechka, G. J. Kabo, A. V. Blokhin, A. S. Shaplov, E. I. Lozinskaya, D. G. Golovanov, K. A. Lyssenko, A. A. Korlyukov, Y. S. Vygodskii, *J. Phys. Chem. B* **2009**, *113*, 9538.
- [23] Y. Umebayashi, J. C. Jiang, Y. L. Shan, K. H. Lin, K. Fujii, S. Seki, S.-I. Ishiguro, S. H. Lin, H. C. Chang, *J. Chem. Phys.* **2009**, *130*, 1234503.
- [24] T. Buffeteau, J. Grondin, J.-C. Lassègues, *Appl. Spectrosc.* **2010**, *64*, 112.
- [25] V. Kempter, B. Kirchner, *J. Mol. Struct.* **2010**, *972*, 22.
- [26] A. Dominguez-Vidal, N. Kaun, M. J. Ayora-Cañada, B. Lendl, *J. Phys. Chem. B* **2007**, *111*, 4446.
- [27] K. Fumino, A. Wulf, R. Ludwig, *Angew. Chem. Int. Ed.* **2008**, *47*, 3830.
- [28] K. Fumino, A. Wulf, R. Ludwig, *Angew. Chem. Int. Ed.* **2008**, *47*, 8731.
- [29] T. Köddermann, K. Fumino, R. Ludwig, J. N. Canongia Lopes, A. A. H. Pádua, *ChemPhysChem* **2009**, *10*, 1181.
- [30] A. Wulf, K. Fumino, R. Ludwig, P. F. Taday, *ChemPhysChem* **2010**, *11*, 349.
- [31] A. Wulf, K. Fumino, R. Ludwig, *Angew. Chem. Int. Ed.* **2010**, *49*, 449.
- [32] T. Buffeteau, J. Grondin, Y. Danten, J.-C. Lassègues, *J. Phys. Chem. B* **2010**, *114*, 7587.
- [33] K. Fumino, A. Wulf, S. P. Verevkin, A. Heintz, R. Ludwig, *ChemPhysChem* **2010**, *11*, 1623.
- [34] C. Daguene, P. J. Dyson, I. Krossing, A. Oleinikova, J. Slattey, C. Wakai, H. Weingartner, *J. Phys. Chem. B* **2006**, *110*, 12682.
- [35] K. Yamamoto, M. Tani, M. Hangyo, *J. Phys. Chem. B* **2007**, *111*, 4854.
- [36] R. Buchner, G. Hefter, *Phys. Chem. Chem. Phys.* **2009**, *11*, 8984.
- [37] I. E. Izgorodina, M. Forsyth, D. R. MacFarlane, *Phys. Chem. Chem. Phys.* **2009**, *11*, 2452.
- [38] K. Nakamura, T. Shikata, *ChemPhysChem* **2010**, *11*, 285.
- [39] H. C. Chang, J. C. Jiang, Y. C. Liou, C. H. Hung, T. Y. Lai, S. H. Lin, *J. Chem. Phys.* **2008**, *129*, 044506.
- [40] H. C. Chang, J. C. Jiang, C. Y. Chang, J. C. Su, C. H. Hung, Y. C. Liou, S. H. Lin, *J. Phys. Chem. B* **2008**, *112*, 4351.
- [41] Y. Umebayashi, J. C. Jiang, S. H. Lin, Y. L. Shan, K. Fujii, S. Seki, S.-I. Ishiguro, S. H. Lin, H. C. Chang, *J. Chem. Phys.* **2009**, *131*, 234502.
- [42] J.-C. Lassègues, J. Grondin, D. Cavagnat, P. Johansson, *J. Phys. Chem. A* **2009**, *113*, 6419.
- [43] A. Wulf, K. Fumino, R. Ludwig, *J. Phys. Chem. A* **2010**, *114*, 685.
- [44] J.-C. Lassègues, J. Grondin, D. Cavagnat, P. Johansson, *J. Phys. Chem. A* **2010**, *114*, 687.
- [45] T. L. Amyes, S. T. Diver, J. P. Richard, F. M. Rivas, K. Toth, *J. Am. Chem. Soc.* **2004**, *126*, 4366.
- [46] R. Giernoth, D. Bankman, *Tetrahedron Lett.* **2006**, *47*, 4293.
- [47] R. Giernoth, D. Bankman, *Eur. J. Org. Chem.* **2008**, 2881.
- [48] P. C. Trulove, R. A. Osteryoung, *Inorg. Chem.* **1992**, *31*, 3980.
- [49] S. T. Handy, M. Okello, *J. Org. Chem.* **2005**, *70*, 1915.
- [50] C. Hardacre, J. D. Holbrey, S. E. J. McMath, *Chem. Commun.* **2001**, 367.
- [51] M. J. Frisch, G. W. Trucks, H. B. Schlegel, G. E. Scuseria, M. A. Robb, J. R. Cheeseman, J. A. Montgomery Jr, T. Vreven, K. N. Kudin, J. C. Burant, J. M. Millam, S. S. Iyengar, J. Tomasi, V. Barone, B. Mennucci, M. Cossi, G. Scalmani, N. Rega, G. A. Petersson, H. Nakatsuji, M. Hada, M. Ehara, K. Toyota, R. Fukuda, J. Hasegawa, M. Ishida, T. Nakajima, Y. Honda, O. Kitao, H. Nakai, M. Klene, X. Li, J. E. Knox, H. P. Hratchian, J. B. Cross, V. Bakken, C. Adamo, J. Jaramillo, R. Gomperts, R. E. Stratmann, O. Yazyev, A. J. Austin, R. Cammi, C. Pomelli, J. W. Ochterski, P. Y. Ayala, K. Morokuma, G. A. Voth, P. Salvador, J. J. Dannenberg, V. G. Zakrzewski, S. Dapprich, A. D. Daniels, M. C. Strain, O. Farkas, D. K. Malick, A. D. Rabuck, K. Raghavachari, J. B. Foresman, J. V. Ortiz, Q. Cui, A. G. Baboul, S. Clifford, J. Cioslowski, B. B. Stefanov, G. Liu, A. Liashenko, P. Piskorz, I. Komaromi, R. L. Martin, D. J. Fox, T. Keith, M. A. Al-Laham, C. Y. Peng, A. Nanayakkara, M. C. Challacombe, P. M. W. Gill, B. Johnson, W. Chen, M. W. Wong, C. Gonzalez, J. A. Pople, *Gaussian 03, Revision E.01*, Gaussian, Inc.: Wallingford, **2004**.
- [52] C. Lee, W. Yang, R. G. Parr, *Phys. Rev. B* **1988**, *37*, 785.
- [53] A. D. Becke, *J. Chem. Phys.* **1993**, *98*, 5648.
- [54] V. Barone, *J. Chem. Phys.* **2005**, *122*, 014108.
- [55] A. Allouche, B. Pourcin, *Spectrochim. Acta* **1993**, *49A*, 571.
- [56] A. M. Belloq, C. Garrigou-Lagrange, *Spectrochim. Acta* **1971**, *27A*, 1091.
- [57] K. Nakamoto, *Infrared and Raman Spectra of Inorganic and Coordination Compounds* (5th edn), Wiley: New York, **1997**.
- [58] M. Chabanel, D. Legoff, K. Touaj, *J. Chem. Soc. Faraday Trans.* **1996**, *92*, 4199.
- [59] C. M. Burba, R. Frech, *J. Phys. Chem. B* **2005**, *109*, 5161.
- [60] S. Tsuzuki, H. Tokuda, K. Hayamizu, M. Watanabe, *J. Phys. Chem. B* **2005**, *109*, 16474.
- [61] S. Tsuzuki, H. Tokuda, M. Mikami, *Phys. Chem. Chem. Phys.* **2007**, *9*, 4780.
- [62] R. Katoh, M. Hara, S. Tsuzuki, *J. Phys. Chem. B* **2008**, *112*, 15426.
- [63] H. Weingartner, *Angew. Chem.* **2008**, *47*, 654.
- [64] P. A. Hunt, B. Kirchner, T. Welton, *Chem. Eur. J.* **2006**, *12*, 6762.
- [65] J. Thar, M. Brehm, A. P. Seitsonen, B. Kirchner, *J. Phys. Chem. B* **2009**, *113*, 15129.
- [66] Y. Yasaka, C. Wakai, N. Matubayasi, M. Nakahara, *J. Phys. Chem. A* **2007**, *111*, 541.
- [67] R. C. Remsing, J. L. Wildin, A. L. Rapp, G. Moyna, *J. Phys. Chem. B* **2007**, *111*, 11619.
- [68] A. Elaiwi, P. B. Hitchcock, K. R. Seddon, N. Srinivasan, Y. M. Tan, T. Welton, J. A. Zora, *J. Chem. Soc. Dalton Trans.* **1995**, 3467.
- [69] Y. Danten, I. Cabaço, M. Besnard, *J. Phys. Chem. A* **2009**, *113*, 2873.
- [70] K. Angenendt, P. Johansson, *J. Phys. Chem. C* **2010**, in press.